ANTIOXIDANTS & REDOX SIGNALING
Volume 9, Number 4, 2007

DOI: 10.1089/ars.2006.1389

Original Research Communication

Characterization of *In Vivo* Tissue Redox Status, Oxygenation, and Formation of Reactive Oxygen Species in Postischemic Myocardium

XUEHAI ZHU,[1,2] LI ZUO,[1] ARTURO J. CARDOUNEL,[1]
JAY L. ZWEIER,[1] and GUANGLONG HE[1]

ABSTRACT

The current study aims to characterize the alterations of *in vivo* tissue redox status, oxygenation, formation of reactive oxygen species (ROS), and their effects on the postischemic heart. Mouse heart was subjected to 30 min LAD occlusion, followed by 60 min reperfusion. *In vivo* myocardial redox status and oxygenation were measured with electron paramagnetic resonance (EPR). *In vivo* tissue NAD(P)H and formation of ROS were monitored with fluorometry. Tissue glutathione/glutathione disulfide (GSH/GSSG) levels were detected with high-performance liquid chromatography (HPLC). These experiments demonstrated that tissue reduction rate of nitroxide was increased 100% during ischemia and decreased 33% after reperfusion compared to the nonischemic tissue. There was an overshoot of tissue oxygenation after reperfusion. Tissue NAD(P)H levels were increased during and after ischemia. There was a burst formation of ROS at the beginning of reperfusion. Tissue GSH/GSSG level showed a 48% increase during ischemia and 29% decrease after reperfusion. In conclusion, the hypoxia during ischemia limited mitochondrial respiration and caused a shift of tissue redox status to a more reduced state. ROS generated at the beginning of reperfusion caused a shift of redox status to a more oxidized state, which may contribute to the postischemic myocardial injury. *Antioxid. Redox Signal.* 9, 447–455.

INTRODUCTION

Myocardial ischemia and acute infarction arise secondary to atherosclerosis, followed by plaque rupture and thrombosis. Current treatments aim to terminate ischemia by re-establishing blood flow as soon as possible. However, reperfusion may cause new damage, reperfusion injury, to the area at risk (7, 21, 28). Several mechanisms have been proposed, such as rapid entry of sodium ions and water into myocardial cells producing intracellular edema during ischemia. Rapid entry of calcium ions produces the contraction bands and mitochondrial granules. Loss of vascular integrity results in hemorrhage into the infarct. Finally, the production of reactive oxygen species (ROS) is responsible for the peroxidation of membrane lipids and disruption of membrane integrity (45, 46). Further, ischemia and reperfusion may alter the myocardial redox status and therefore the ability to detoxify ROS. In postischemic myocardium, increased generation of nitric oxide (NO) and superoxide ($O_2^{\bullet -}$) occurs, resulting in formation of peroxynitrite ($ONOO^-$), and these reactive nitrogen species (RNS) have been reported to suppress oxygen consumption on mitochondrial respiratory chain (38, 40).

It has been demonstrated that NO generated from endothelial NO synthase (eNOS) inhibits mitochondrial respiration

[1]Center for Biomedical EPR Spectroscopy and Imaging, Davis Heart and Lung Research Institute, and the Division of Cardiovascular Medicine, Department of Internal Medicine, The Ohio State University College of Medicine, Columbus, Ohio.
[2]Key Laboratory of Organ Transplantation, Ministry of Education Institute of Organ Transplantation, Tongji Hospital, Tongji Medical College, Huazhong University of Science and Technology, Wuhan, China.

by ONOO⁻ mediated nitration of complex I and IV (18, 19, 34, 36, 37, 40). The inhibited mitochondrial respiration increases tissue oxygenation (PO_2) after reperfusion (40). This increased tissue PO_2 may potentiate the increase of ROS through electron leakage on mitochondrial respiratory chain (10, 20, 23, 25, 29, 35). On the other hand, mitochondrial respiration controls tissue redox balance by controlling the utilization of reduced substrates such as NAD(P)H. Inhibition of electron flux of mitochondrial subcomponents will switch cellular redox status to a more reduced state with excessive accumulation of NAD(P)H (4, 8, 20). This reduced state may also potentiate formation of ROS/RNS upon reoxygenation (2, 15, 44). Therefore, alterations in tissue redox status, oxygenation, and formation of ROS/RNS occur in ischemic and reperfused myocardium and are of central importance in the pathogenesis of postischemic injury.

Therefore, there is a need of *in vivo* techniques to measure tissue redox status, oxygenation, and formation of ROS. Several other techniques, such as cytochrome c reduction and lucigenin-enhanced chemiluminescence, lack the potential of *in vivo* capability. We used localized electron paramagnetic resonance (EPR) spectroscopy to measure *in vivo* tissue redox status and tissue PO_2 by introducing bioreducible spin probe nitroxide (11, 13, 33, 40, 47) and oxygen-sensitive probe lithium phthalocyanine (LiPc) (14, 17, 31). EPR spectroscopy has advantages over other techniques. The implanted/injected probes can move freely with the beating heart, and myocardial redox status and PO_2 can be monitored repetitively after the chest is closed (40). We used localized fluorometry to measure *in vivo* tissue NAD(P)H level and formation of ROS (30, 39, 41). Autofluorescence spectroscopy is an accepted method for measuring NAD(P)H in isolated hearts and myocardial tissue (5, 22, 26, 30). The majority of measured NAD(P)H is believed to originate from the tricarboxylic acid cycle (TCA) (3, 9, 22). This technique has been used to monitor relative NAD(P)H concentration and thus mitochondrial redox status. The dye hydroethidine (HE) is a noncharged fluorescent probe specifically sensitive to $O_2^{\bullet -}$, ONOO⁻, and hydroxyl radical (·OH) but not to H_2O_2 (1, 6). After reacting with $O_2^{\bullet -}$, HE forms oxyethidine and probably by reacting with other oxidants to form ethidine (ET) (39).

Finally, with localized *in vivo* EPR spectroscopy and fluorometry, we demonstrated that while tissue oxygenation was limited as in ischemia, tissue redox status shifted to reduced state, tissue formation of ROS was low, and tissue NAD(P)H content was high. Upon reperfusion, tissue redox status shifted to oxidized state, tissue formation of ROS was high, and tissue NAD(P)H content was low. The elevated level of NAD(P)H during ischemia and hyperoxygenation after reperfusion may potentiate the burst formation of ROS that may contribute to the postischemic myocardial injury.

MATERIALS AND METHODS

Animals

Male C57BL/6 mice were purchased from Jackson Laboratory (Bar Harbor, Me). All surgery procedures were performed with the approval of the Institutional Animal Care and Use Committee at The Ohio State University, Columbus, Ohio, and conformed to the Guide for the Care and Use of Laboratory Animals (NIH publication No. 86–23, revised 1985).

In vivo *ischemia reperfusion mouse model*

The *in vivo* ischemia reperfusion mouse model was performed with a technique similar to that described previously (40). Mice were anesthetized with ketamine (55 mg/kg) plus xylazine (15 mg/kg). Atropine (0.05 mg SC) was administered to reduce airway secretion. Animals were intubated and ventilated with room air (tidal volume 250 μl, 120 breath/min) with a mouse respirator (Harvard Apparatus, Holliston, MA). Rectal temperatures were maintained at 37°C by a thermo heating pad. After thoracotomy, the left anterior descending (LAD) coronary artery was ligated with an 8–0 silk suture. After 30 min of ischemia, the occlusion was released, and reperfusion was confirmed visually.

To further confirm the LAD occlusion, myocardial tissue blood flow was monitored. After thoracotomy, an optic suction probe (P10d, Moor Instruments, Wilmington, DE) connected to a laser Doppler perfusion monitor (Moor Instruments) was placed on the area at risk and blood flow was monitored before, during, and after coronary occlusion (40).

Measurement of in vivo *tissue redox status with localized EPR*

In vivo EPR measurements of tissue redox status were performed using 2,2,5,5-tetramethyl-3-carboxylpyrrolidine-*N*-oxyl (PCA) (Sigma Chemical Co., Milwaukee, WI) as the spin probe with a three-line EPR spectrum. The nitroxide solutions were prepared in PBS and kept frozen until use. About 5 μl 10 m*M* PCA solution was intramuscularly injected as a bolus into the area at risk. Then EPR spectra were acquired before, during, and after ischemia with a surface loop resonator placed on top of the heart. The lower field peak-height was monitored with time to determine the rate of reduction.

In vivo *localized EPR oximetry*

Lithium phthalocyanine (LiPc) was used as the probe for EPR oximetry (13, 32). The O_2 response of LiPc showed good linearity from 0 to 150 mm Hg with a sensitivity of 7.25 mG/mm Hg. After thoracotomy and exposure of the heart, ~10 μg of LiPc crystals loaded in a 27-gauge needle was implanted into the mid-myocardium in the area at risk. After 30 min equilibration, the mouse was placed into the custom-made L-band EPR spectrometer with its heart under the resonator loop (12). EPR spectra of LiPc crystals were acquired with following parameters: frequency 1.1 GHz, microwave power 16 mW, modulation field 0.0045 mT, and scan width 0.2 mT. The position of the implanted crystals was confirmed by histology.

In vivo *fluorescence measurement of tissue NAD(P)H content*

In vivo autofluorescence of the sum of tissue NADH and NADPH, NAD(P)H, in the area at risk were measured within a black box that excluded the ambient light (30). A 6-mm diameter fiberoptic bundle that contained both excitation and emission fibers was carefully positioned adjacent to and directed toward the area at risk. To avoid noise from other organs, the whole body of the mouse was covered with a black cloth with one small opening (3 × 3 mm) at the area at risk. The proximal end of the fiberoptic cable was connected to a ratiometric fluorometer (Radnoti Glass, Monrovia, CA). Fluorescence was excited using a 150-W xenon arc lamp filtered through one of four alternating excitation filters. A single excitation filter with a specific designated ultraviolet range was used to excite NAD(P)H at 330 nm with a band width of 80 nm. The emission range for NAD(P)H was 470 ± 5 nm. The signals were averaged over 5 sec, recorded and graphed using a modified program (IOTECH with software from Strawberry Tree, Cleveland, OH).

HPLC analysis of NAD(P)H levels

To quantify NAD(P)H levels measured from autofluorescence, HPLC analysis of tissue NAD(P)H levels were followed on tissues collected from the area at risk before ischemia, at the end of 25 min ischemia, and at the end of 20 min reperfusion. Then heart samples were ground to fine powder under liquid nitrogen and extracted and homogenized in ice-cold perchloric acid (0.4 mol/L). The denatured protein was pelleted and reserved for protein analysis. The acid extract was neutralized with equal volumes of 0.4 mol/L $KHCO_3$. Each extract was subjected to nucleotide analysis using gradient ion-pair reversed-phase liquid chromatography. HPLC separation was performed using an ESA (Chelmsford, MA) solvent delivery system with a 3-μm symmetry C18 column (3.9 x 150 mm inner diameter, Waters Corporation, Milford, MA). Separation was performed by reverse-phase chromatography using an isocratic mobile phase consisting of buffer A (35 mmol/L KH_2PO_4, 6 mmol/L tetrabutylammonium hydrogensulfate, pH 6.0, 125 mmol/L ethylenediaminetetraacetic acid) and buffer B (a mixture of buffer A and HPLC-grade acetonitrile in a ratio of 1:1, vol/vol), filtered through a 0.2-μm membrane filter and helium degassed. The flow rate was set at 1.0 ml/min and detection was performed at 260 nm using an ESA variable wavelength UV/V absorbance detector.

In vivo *localized fluorescence measurement of ROS*

HE stock solution was made in *N,N*-dimethylacetamide (Acros Organics, Morris Plains, NJ). About 20 μl 200 μ*M* HE in PBS solution was injected intramuscularly as a bolus into the area at risk 5 min before ischemia. The fluorescence measurements were followed immediately after the injection. The ET excitation filter was set at 515 ± 20 nm, and the ET emission at 590 ± 25 nm.

HPLC measurement of tissue GSH/GSSG

At the end of 30 min ischemia and 60 min reperfusion, animals were euthanized and myocardial tissue in the area at risk were excised and weighed. Heart tissue was ground in liquid nitrogen and homogenized in 0.5 ml 200 m*M* methanesulfonic acid containing 5 m*M* diethylenetriaminepentaacetic acid (pH < 2.0) using a Dounce glass homogenizer. Then tissue homogenate was centrifuged for 30 min at 14,000 rpm at 4°C. The supernatant was diluted 1:1 with mobile phase and stored frozen at -80°C for GSH assay. The GSH assays were performed with HPLC (16). Samples were separated on a Polaris 5 μm, 0.4 x 20 cm C-18 column eluted with a mobile phase of 50 m*M* NaH_2PO_4, 0.05 m*M* octanesulfonic acid, and 2% acetonitrile adjusted to pH 2.7 with phosphoric acid and a flow rate of 1 ml/min. An ESA CoulArray detector was used with the guard cell set at +950 mV, electrode 1 at +400 mV, and electrode 2 at +880 mV. Full-scale output was set at 100 μA and peak areas were analyzed using the CoulArray software (ESA, Chelmsford, MA). A standard curve was obtained using a 10 μ*M*-to-1 m*M* solution of GSH, from which GSH concentrations were determined. The GSH values were expressed as nmols/g of tissue wet weight.

Measurement of myocardial hemodynamics and infarct size

After anesthesia, the right common carotid artery was cannulated with a 1.4F Millar tip transducer catheter (model SPR-261) connected to a PowerLab (ADInstruments, Inc., Colorado Springs, CO) system for monitoring of mean arterial blood pressure (MABP) and heart rate (HR). Rate pressure product (RPP) was calculated as: RPP = MABP × HR (mm Hg/min). In all groups, similar basal heart rates were observed with values around 300 bpm, typical for anesthetized mice.

To measure the infarct size, mouse heart was subjected to 30 min LAD occlusion and 24 h reperfusion. Then mice were reventilated and LAD was reoccluded. About 1.5 ml of 4.0% Evans blue (Sigma) was injected from the inferior vena cave to delineate the nonischemic myocardium from that of the ischemic myocardium. Then mice were euthanized and hearts were excised and cut into four transverse slices. The slices were stained with 1.5% 2,3,5-triphenyltetrazolium chloride (TTC, Sigma) to determine the infarct area (NEC). Then the slices were photographed under a microscope (Nikon) to determine area of LV, area at risk (AAR), and NEC by computerized planimetry. Infarct size was expressed as percentage of the AAR in LV.

Statistical analysis

Two-way ANOVA was used for data analysis of blood flow, reduction rate of nitroxide, PO_2, NAD(P)H level, and GSH/GSSG levels followed by Newman–Keuls multiple-comparison test among the groups. Data were represented as mean ± SEM. A value of $p < 0.05$ was considered significant.

RESULTS

In vivo *myocardial tissue reduction capability*

After injection of PCA into the area at risk, EPR spectrum before, during, and after ischemia was collected every 60 sec for up to 1 h. The peak-height of the lowest field EPR line was monitored with time. The time-dependent profile of the EPR signal is shown in Fig. 1 as the open circles. A faster

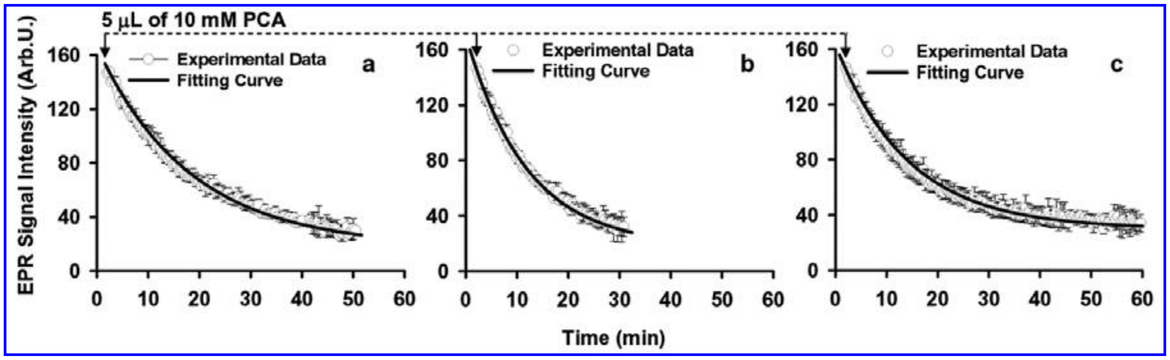

FIG. 1. *In vivo* measurement of tissue reduction rate of PCA. After thoracotomy and exposure of the heart, 5 μl of 10 m*M* PCA PBS solution was injected into the area at risk and EPR spectroscopy was followed. The decay of EPR signal intensity was shown as the *open circles,* while the single exponential decay fitting curves were shown as the *solid lines*: (**a**) before (0.042 ± 0.004/min); (**b**) during (0.084 ± 0.015/min); (**c**) after (0.028 ± 0.004/min) 30 min LAD occlusion; $n = 7$.

decay of the EPR signal was observed in the ischemic tissue and a slower decay was observed in the postischemic tissue compared to that of the preischemic tissue.

To confirm that the decay of EPR signal was due to the reduction of the applied probe, 5 μl 10 m*M* potassium ferricyanide ($K_3Fe(CN)_6$) was injected to the same spot 10 min after the injection of PCA. $K_3Fe(CN)_6$ was a known standard oxidant to oxidize the reduced form of PCA, hydroxylamine, back to its nitroxide form. It was observed that after injection of $K_3Fe(CN)_6$, nearly 90% of the reduced PCA signal was restored (Fig. 2). This confirmed that the decay of PCA signal was mainly due to tissue reduction of this probe.

Then the decay of EPR signal intensity was fitted with a single exponential curve as the solid line shown in Fig. 1. The reduction rate constants of PCA in the preischemic, ischemic, and postischemic myocardium in the area at risk were 0.042 ± 0.004, 0.084 ± 0.015, and 0.028 ± 0.004 min^{-1} as shown in Fig. 3.

In vivo *myocardial tissue* PO_2

After LAD occlusion, tissue blood flow was decreased to 14.4 ± 3.9% at the end of 30 min ischemia compared to preischemic value. Upon reperfusion, blood flow was restored to 68.8 ± 5.4% of the baseline level during the first 5 min reperfusion. This indicated that there was no reactive hyperemia after reperfusion.

As shown in Fig. 4, the baseline tissue PO_2 was measured as 16.4 ± 0.7 mm Hg. At the end of 30 min ischemia, tissue PO_2 dropped to 1.0 ± 0.2 mm Hg. Upon reperfusion, there was an overshoot of tissue PO_2 in the first 12 min (33.1 ± 2.8 mm Hg) followed by a slight increase to a level of 38.3 ± 0.6 mm Hg at the end of 60 min reperfusion. Interestingly, the level of tissue PO_2 corresponded inversely to tissue reduction rate of PCA:low PO_2 to fast reduction, high PO_2 to slow reduction.

Variation of tissue NAD(P)H levels

Tissue NAD(P)H level was increased from 38.3 ± 4.5 nmol/mg protein before ischemia to 90.0 ± 9.6 nmol/mg protein at the end of 25 min ischemia, and 50.9 ± 6.5 nmol/mg protein after 20 min reperfusion (Fig. 5). This data, together with the measurement of redox status, strongly suggest that during ischemia, tissue redox status shifted to a reducing state, which could be due to high tissue NAD(P)H content and low tissue PO_2.

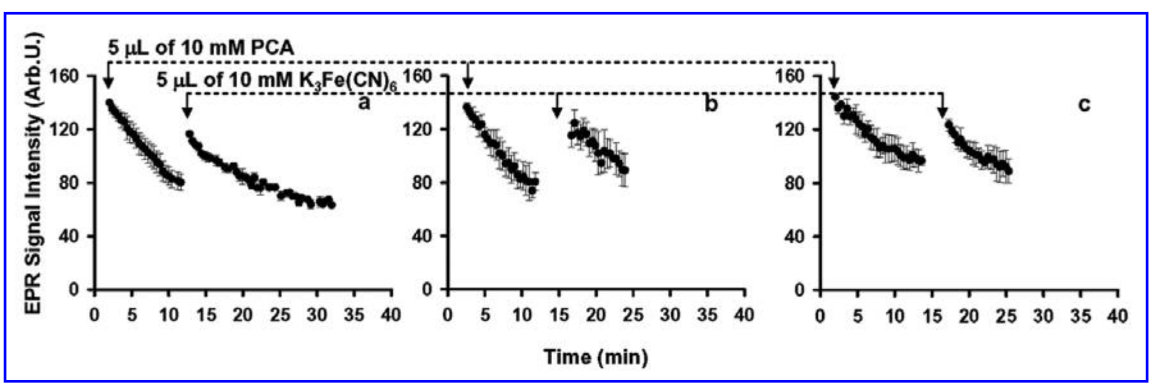

FIG. 2. *In vivo* measurement of the reappearance of EPR signal. About 5 μl 10 m*M* $K_3Fe(CN)_6$ was injected intramuscularly to the same spot 10 min after the injection of PCA (**a**) before, (**b**) during, and (**c**) after 30 min LAD occlusion. Restoration of the decayed EPR signal was observed; $n = 7$.

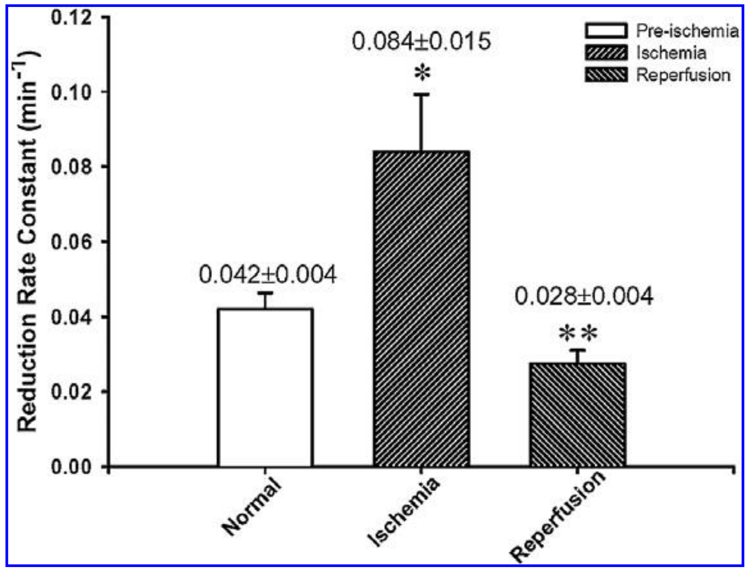

FIG. 3. Reduction rate constants of PCA. The decay of EPR signal in Fig. 2 was fitted with a single exponential decay curve to obtain the reduction rate constants of PCA (**a**) before, (**b**) during, and (**c**) after LAD occlusion; $n = 7$. *ischemia *vs.* normal, $p < 0.01$; **reperfusion *vs.* normal, $p < 0.01$.

Alterations of the formation of ROS in the area at risk

As shown in Fig. 6, there was a small peak (peaked at 7.5 min with a peak value of 1.07 ± 0.02 of the baseline) observed during the first 5 min of ischemia and it was decreased to baseline level after the burst. Upon reperfusion, a larger peak was observed for a period of 7 min, with a peak value of 1.24 ± 0.20 of the baseline.

Tissue GSH/GSSG levels in the postischemic myocardium

GSH/GSSG level was increased 48% in the ischemic myocardium and decreased 29% in the postischemic myocardium compared to that of the preischemic tissue (Fig. 7 and Table 1). This data confirmed that tissue redox status shifted to a reducing state in the ischemic myocardium and to an oxidized state in the postischemic myocardium.

Measurements of myocardial hemodynamics and infarct size

Myocardial RPP was considered as an index of cardiac tissue oxygen demand. As shown in Fig. 8A, myocardial RPP was decreased slightly from a value of 20.2 ± 2.3 x 10^3 mmH/min before ischemia to 16.2 ± 2.1 × 10^3 mmH/min after 60 min reperfusion. However, the difference was not significant since RPP represented the global function of the heart, while the ischemic injury in our study was only in the area at risk. The measurement of hemodynamics indicated that the postischemic myocardial injury was only partially manifested by the global function of the heart such as RPP. Infarct size was measured as 31.0 ± 2.5 % of the AAR 24 h after reperfusion (Fig. 8B).

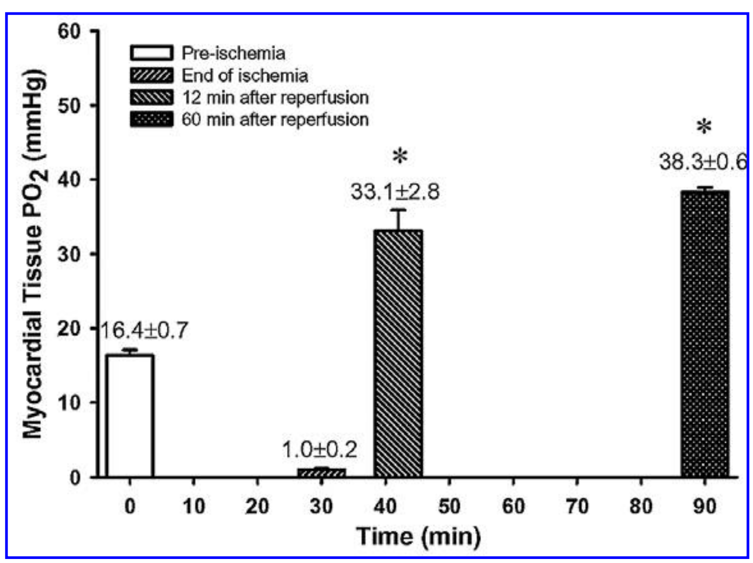

FIG. 4. Alterations of *in vivo* tissue PO_2 in the area at risk. After thoracotomy and exposure of the heart, about 10 μg of LiPc crystals were implanted into the mid-myocardium. After 30 min equilibration, EPR spectrum of LiPc was acquired. Tissue PO_2 was measured as 16.4 ± 0.7 mm Hg before ischemia, 1.0 ± 0.2 mm Hg at the end of 30 min ischemia, 33.1 ± 2.8 mm Hg at 12 min reperfusion, and 38.3 ± 0.6 mm Hg at 60 min reperfusion. $N = 7$, * reperfusion *vs.* preischemia, $p < 0.01$.

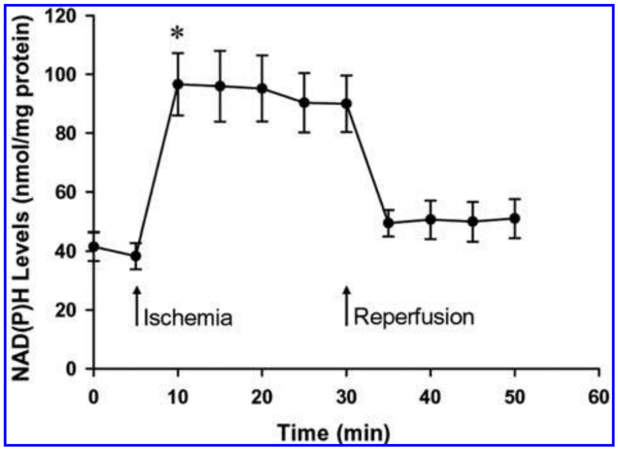

FIG. 5. Fluorescence and HPLC measurements of tissue NAD(P)H content in the area at risk. Tissue NAD(P)H level was increased from 38.3 ± 4.5 nmol/mg protein before ischemia to 90.0 ± 9.6 nmol/mg protein at the end of ischemia, and 50.9 ± 6.5 nmol/mg protein after reperfusion. $N = 4$, *ischemia *vs.* preischemia, $p < 0.05$.

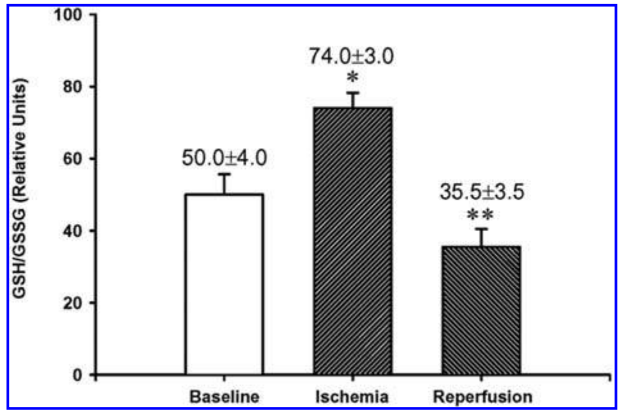

FIG. 7. Measurements of tissue GSH/GSSG level with HPLC. Myocardial tissues in the area at risk were excised before ischemia, at the end of 30 min ischemia, and at the end of 60 min reperfusion. Then HPLC measurements were followed. GSH/GSSG level was increased from 50.0 ± 4.0 to 74.0 ± 3.0 (48% increase) and decreased to 35.5 ± 3.5 (29% decrease) in the preischemic, ischemic, and postischemic myocardium. $N = 4$, *ischemia *vs.* baseline, $p < 0.05$; **reperfusion *vs.* baseline, $p < 0.05$.

DISCUSSION

In summary, tissue reduction rate of nitroxide was increased 100% during ischemia and decreased 33% after reperfusion compared to baseline level. Tissue PO_2 dropped to 1.0 ± 0.2 mm Hg at the end of 30 min ischemia and overshot to a level of 33.1 ± 2.8 mm Hg in the first 12 min of reperfusion and 38.3 ± 0.6 mm Hg at the end of 60 min reperfusion. Tissue NAD(P)H level was increased from 38.3 ± 4.5 nmol/mg protein before ischemia to 90.0 ± 9.6 nmol/mg protein at the end of ischemia, and 50.9 ± 6.5 nmol/mg protein after reperfusion. A small burst of ROS during the first 5 min of ischemia and a large burst upon reperfusion were observed. Since fluorescence measured only the production of ET, the oxidized form of HE, the peak at the beginning of reperfusion indicated that there was a burst formation of ROS. Total tissue GSH/GSSG level was increased 48% at the end of 30 min ischemia and decreased 29% at the end of 60 min reperfusion.

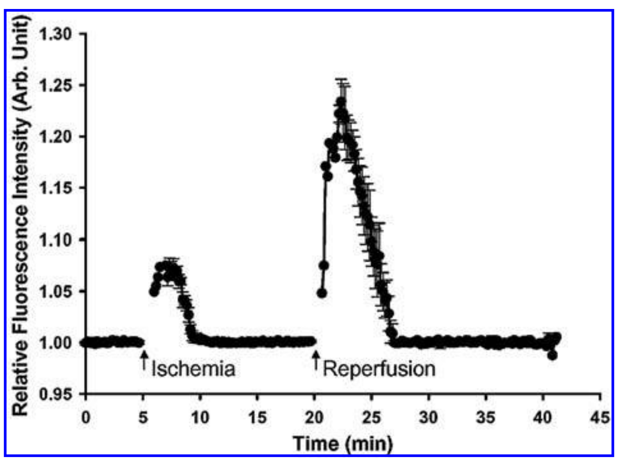

FIG. 6. ***In vivo*** **measurements of the burst formation of ROS with fluorometry.** After thoracotomy and exposure of the heart, 20 μl of 200 μ*M* HE injected intramuscularly in the area at risk 5 min before ischemia. Then fluorescence was measured before ischemia, during 15 min LAD occlusion, and after reperfusion. The measurements were repeated on 4 animals and the averaged results are shown in the figure. There appeared a burst formation of fluorescence signal within the first 5 min of ischemia. Upon reperfusion, there was another larger burst of fluorescence signal.

During ischemia, there was a lack of O_2 and nutrients to the tissue. Therefore, the mitochondrial respiration was limited, leading to the accumulation of NAD(P)H. It was very interesting to notice that there was a small burst of ROS at the beginning of ischemia. With data presented in the current study, we can not definitively derive a mechanism to explain how ischemia may trigger this burst formation of $O_2^{\bullet-}$. However, one of the possibilities could be that as an electron donor, the fast accumulation of NAD(P)H at the beginning of ischemia might be able to potentiate a burst of $O_2^{\bullet-}$ given still sufficient O_2 at the onset of ischemia. The detailed mechanism responsible for this small burst formation of ROS is warranted in the future studies.

Upon reperfusion, there was a burst of ROS and possibly also RNS, which exerted a suppressive regulation on the mitochondrial respiration and caused the hyperoxygenation status in the tissue (40). The hyperoxygenation would further potentiate more $O_2^{\bullet-}$ generation after reperfusion. Therefore, the burst of ROS/RNS would render the tissue to a more oxidative status. Under this oxidative insult, tissue antioxidant defense system(s), such as glutathione, participated in the detoxification of the insults (24, 27). This led to the high level of GSH/GSSG during ischemia and low level of GSH/GSSG after reperfusion. Myocardial hemodynamics

TABLE 1. GSH AND GSSG LEVELS IN THE MYOCARDIUM

	Control	*Ischemia*	*Reperfusion*
GSH (nmols/g protein)	65.0 ± 2.6	111.0 ± 3.3*	53.5 ± 1.9†
GSSG (nmols/g protein)	1.3 ± 0.1	1.5 ± 0.1	1.5 ± 0.1

*Ischemia *vs.* control, $p < 0.05$; †reperfusion *vs.* control, $p < 0.05$.

showed a slightly decreased cardiac function after reperfusion. The reperfusion injury in the postischemic myocardium as indicated by the injured myocardium was only partially manifested by this global cardiac function. ROS/RNS after reperfusion could be one of the causative factors to the postischemic myocardial injury. Therefore, with this array of techniques, we were able to measure a series of important parameters such as *in vivo* tissue redox status, *in vivo* tissue oxygenation, *in vivo* NAD(P)H levels, and *in vivo* ROS formation. With these measurements, we suggest that the burst formation of ROS after reperfusion may act as a causative factor to the hyperoxygenation status in the tissue thereby to the postischemic myocardial injury (40). The injury caused by the burst formation of ROS was converged on the degradation of mitochondrial enzymes (40).

One of the challenges in measuring tissue redox status is to find an appropriate index to indicate the nonequilibrated/time-dependent characteristics. NAD(P)H was reported to be a redox indicator during myocardial ischemia/reperfusion (2, 41–43). However, our data demonstrated that NAD(P)H level was higher in the postischemic state than that in the preischemic state and this would imply that the redox status was still on the reducing side after reperfusion if NAD(P)H was considered as the redox indicator. Therefore, NAD(P)H can only be considered as a redox indicator during the nonequilibrated ischemic period. Formation of ROS was also considered as an indicator of redox status. Again our data indicated that even during ischemia there was a burst of ROS, which would imply that the tissue redox status was on the oxidative side during ischemia. Therefore, ROS can only be considered as a redox indicator during the nonequilibrated reperfusion period. These data may reflect the nonequilibration of tissue redox status and oxygenation during ischemia and reperfusion. However, if we take both NAD(P)H and ROS into consideration, we came to the conclusion that during ischemia, even though there was a burst of ROS, the NAD(P)H level dominated the tissue into the reducing side. Similarly, during reperfusion, even though the NAD(P)H level was slightly higher than that of normal tissue, the larger burst of ROS dominated the tissue into oxidative side. Actually, tissue GSH/GSSG level and reduction rate of nitroxide gave a better indication of the equilibrated tissue redox status.

There were several challenges of using EPR spin probes to measure tissue redox status. One was to determine whether the applied spin probes were reduced or oxidized. Another was to determine the ratio of the reduction versus tissue washout. From the reoxidation experiments, it was clearly shown that the applied spin probes were reduced and the tissue washout was at most 10% of the total applied amount, which was within the range of the standard error (10% of 0.042/min was 0.004/min that was the SE value). The reduction rates of nitroxide were averaged over 30 min due to the requirement of a period of time for the calculation. Therefore, the time resolution was limited in the current experiments. Future study is warranted to design such a redox probe with fast decay rate and high cellular retention to allow redox measurement in a narrow time window. One of the challenges of localized spectroscopy was the limitation to a single point site; therefore results were dependent on tissue heterogeneity. By carefully implanting or injecting the EPR and fluores-

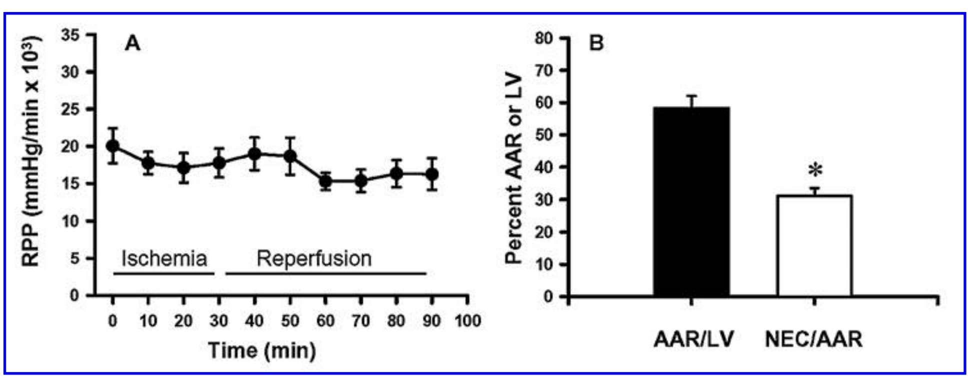

FIG. 8. Measurements of hemodynamics and infarction. HR and MABP were monitored. Then MABP was calculated as: MABP = arterial end diastolic pressure + (arterial systolic pressure – arterial end diastolic pressure)/3. RPP was calculated as: RPP = HR × MABP (**A**). NEC was measured in mice subjected to 30 min LAD occlusion followed by 24 h of reperfusion (**B**). RPP, rate pressure product; MABP, mean arterial blood pressure; HR, heart rate; AAR: area at risk; AAR/LV: area at risk per left ventricular area; NEC/AAR, infarct size per area at risk. $N = 7$, *NEC/AAR *vs.* AAR/LV, $p < 0.05$.

cence probes, one can obtain the localized information from the core of the area at risk. Future development is warranted to image the whole risk area to allow three-dimensional mapping of oxygen and fluorescence intensity.

In conclusion, *in vivo* EPR spectroscopy and fluorometry provided direct evidence of the alterations of tissue redox status, oxygenation, and formation of ROS in the ischemic and reperfused myocardium. The high reduction rate of nitroxide in the ischemic myocardium was consistent with the low tissue PO_2, low level of ROS, high NAD(P)H content, and high level of GSH/GSSG. The low reduction rate of nitroxide in the postischemic myocardium was consistent with the high tissue PO_2, high level of ROS, low NAD(P)H content, and low level of GSH/GSSG. The limited mitochondrial respiration due to hypoxia during ischemia caused an increase of tissue NAD(P)H content and therefore shifted the tissue to a more reduced state. The formation of ROS after reperfusion contributed to the oxidative tissue redox status. The altered redox status and formation of ROS/RNS may eventually contribute to the postischemic myocardial injury.

ACKNOWLEDGMENTS

The authors thank Dr. Thomas Clanton for help with fluorometry, Dr. Ilangovan Govindasamy for help with EPR oximetry, and Dr. Yuanmu Deng for help with data analysis. This work was supported by AHA grant GRT962974, NIH grants HL081630 (GH), HL073087 (CKS), and NIH grants HL63744, HL65608, and HL38324 (JLZ).

ABBREVIATIONS

AAR, area at risk; eNOS, endothelial nitric oxide synthase; EPR, electron magnetic resonance; ET, ethidine; GSH/GSSG, glutathione/glutathione disulfide; HE, hydroethidine; H_2O_2, hydrogen peroxide; HPLC, high-performance liquid chromatography; HR, heart rate; LAD, left anterior descending coronary artery; LV, left ventricle; LiPc, lithium phthalocyanine; MABP, mean arterial blood pressure; NAD(P)H, reduced form of nicotinamide adenine dinucleotide (phosphate); NEC, infarct area; NO, nitric oxide; $O_2^{\bullet -}$, superoxide; $ONOO^-$, peroxynitrite; PCA, 2,2,5,5-tetramethyl-3-carboxylpyrrolidine-*N*-oxyl; PO_2, tissue partial oxygen pressure; ROS, reactive oxygen species; RPP, rate pressure product; TCA, tricarboxylic acid cycle; TTC, 2,3,5-triphenyltetrazolium chloride.

REFERENCES

1. Al–Mehdi AB, Shuman H, and Fisher AB. Intracellular generation of reactive oxygen species during nonhypoxic lung ischemia. *Am J Physiol* 272: L294–300, 1997.
2. Angelos MG, Kutala VK, Torres CA, He G, Stoner JD, Mohammad M, and Kuppusamy P. Hypoxic reperfusion of the ischemic heart and oxygen radical generation. *Am J Physiol Heart Circ Physiol* 290: H341–347, 2006.
3. Barlow CH and Chance B. Ischemic areas in perfused rat hearts: measurement by NADH fluorescence photography. *Science* 193: 909–910, 1976.
4. Beltran B, Mathur A, Duchen MR, Erusalimsky JD, and Moncada S. The effect of nitric oxide on cell respiration: A key to understanding its role in cell survival or death. *Proc Natl Acad Sci USA* 97: 14602–14607, 2000.
5. Brandes R and Bers DM. Increased work in cardiac trabeculae causes decreased mitochondrial NADH fluorescence followed by slow recovery. *Biophys J* 71: 1024–1035, 1996.
6. Budd SL, Castilho RF, and Nicholls DG. Mitochondrial membrane potential and hydroethidine-monitored superoxide generation in cultured cerebellar granule cells. *FEBS Lett* 415: 21–24, 1997.
7. Cannon RO, 3rd. Mechanisms, management and future directions for reperfusion injury after acute myocardial infarction. *Nat Clin Pract Cardiovasc Med* 2: 88–94, 2005.
8. Cleeter MW, Cooper JM, Darley–Usmar VM, Moncada S, and Schapira AH. Reversible inhibition of cytochrome c oxidase, the terminal enzyme of the mitochondrial respiratory chain, by nitric oxide. Implications for neurodegenerative diseases. *FEBS Lett* 345: 50–54, 1994.
9. Eng J, Lynch RM, and Balaban RS. Nicotinamide adenine dinucleotide fluorescence spectroscopy and imaging of isolated cardiac myocytes. *Biophys J* 55: 621–630, 1989.
10. Ferdinandy P and Schulz R. Nitric oxide, superoxide, and peroxynitrite in myocardial ischaemia-reperfusion injury and preconditioning. *Br J Pharmacol* 138: 532–543, 2003.
11. Halpern HJ, Yu C, Peric M, Barth E, Grdina DJ, and Teicher BA. Oxymetry deep in tissues with low-frequency electron paramagnetic resonance. *Proc Natl Acad Sci USA* 91: 13047–13051, 1994.
12. He G, Evalappan SP, Hirata H, Deng Y, Petryakov S, Kuppusamy P, and Zweier JL. Mapping of the B1 field distribution of a surface coil resonator using EPR imaging. *Magn Reson Med* 48: 1057–1062, 2002.
13. Ilangovan G, Liebgott T, Kutala VK, Petryakov S, Zweier JL, and Kuppusamy P. EPR oximetry in the beating heart: myocardial oxygen consumption rate as an index of postischemic recovery. *Magn Reson Med* 51: 835–842, 2004.
14. Ji LL, Fu RG, Waldrop TG, Liu KJ, and Swartz HM. Myocardial response to regional ischemia and reperfusion *in vivo* in rat heart. *Can J Physiol Pharmacol* 71: 811–817, 1993.
15. Klawitter PF, Murray HN, Clanton TL, and Angelos MG. Reactive oxygen species generated during myocardial ischemia enable energetic recovery during reperfusion. *Am J Physiol Heart Circ Physiol* 283: H1656–1661, 2002.
16. Kuppusamy P, Li H, Ilangovan G, Cardounel AJ, Zweier JL, Yamada K, Krishna MC, and Mitchell JB. Noninvasive imaging of tumor redox status and its modification by tissue glutathione levels. *Cancer Res* 62: 307–312, 2002.
17. Liu KJ, Gast P, Moussavi M, Norby SW, Vahidi N, Walczak T, Wu M, and Swartz HM. Lithium phthalocyanine: a probe for electron paramagnetic resonance oximetry in viable biological systems. *Proc Natl Acad Sci USA* 90: 5438–5442, 1993.
18. Lizasoain I, Moro MA, Knowles RG, Darley–Usmar V, and Moncada S. Nitric oxide and peroxynitrite exert distinct effects on mitochondrial respiration which are differentially blocked by glutathione or glucose. *Biochem J* 314: 877–880, 1996.
19. Loke KE, McConnell PI, Tuzman JM, Shesely EG, Smith CJ, Stackpole CJ, Thompson CI, Kaley G, Wolin MS, and Hintze TH. Endogenous endothelial nitric oxide synthase-derived nitric oxide is a physiological regulator of myocardial oxygen consumption. *Circ Res* 84: 840–845, 1999.
20. Moncada S and Erusalimsky JD. Does nitric oxide modulate mitochondrial energy generation and apoptosis? *Nat Rev Mol Cell Biol* 3: 214–220, 2002.
21. Neuzil J, Rayner BS, Lowe HC, and Witting PK. Oxidative stress in myocardial ischaemia reperfusion injury: a renewed focus on a long-standing area of heart research. *Redox Rep* 10: 187–197, 2005.
22. Nuutinen EM. Subcellular origin of the surface fluorescence of reduced nicotinamide nucleotides in the isolated perfused rat heart. *Basic Res Cardiol* 79: 49–58, 1984.
23. Ohnishi ST, Ohnishi T, Muranaka S, Fujita H, Kimura H, Uemura K, Yoshida K, and Utsumi K. A possible site of superoxide generation in the complex I segment of rat heart mitochondria. *J Bioenerg Biomembr* 37: 1–15, 2005.

24. Opstad KS, Provencher SW, Bell BA, Griffiths JR, and Howe FA. Detection of elevated glutathione in meningiomas by quantitative *in vivo* 1H MRS. *Magn Reson Med* 49: 632–637, 2003.
25. Poderoso JJ, Carreras MC, Lisdero C, Riobo N, Schopfer F, and Boveris A. Nitric oxide inhibits electron transfer and increases superoxide radical production in rat heart mitochondria and submitochondrial particles. *Arch Biochem Biophys* 328: 85–92, 1996.
26. Riess ML, Camara AK, Chen Q, Novalija E, Rhodes SS, and Stowe DF. Altered NADH and improved function by anesthetic and ischemic preconditioning in guinea pig intact hearts. *Am J Physiol Heart Circ Physiol* 283: H53–60, 2002.
27. Schafer FQ and Buettner GR. Redox environment of the cell as viewed through the redox state of the glutathione disulfide/glutathione couple. *Free Radic Biol Med* 30: 1191–1212, 2001.
28. Semenza GL. Cellular and molecular dissection of reperfusion injury: ROS within and without. *Circ Res* 86: 117–118, 2000.
29. Sohal RS. Mitochondria generate superoxide anion radicals and hydrogen peroxide. *FASEB J* 11: 1269–1270, 1997.
30. Stoner JD, Angelos MG, and Clanton TL. Myocardial contractile function during postischemic low-flow reperfusion: critical thresholds of NADH and O2 delivery. *Am J Physiol Heart Circ Physiol* 286: H375–380, 2004.
31. Swartz HM, Bacic G, Friedman B, Goda F, Grinberg O, Hoopes PJ, Jiang J, Liu KJ, Nakashima T, O'Hara J, and et al. Measurements of pO2 in vivo, including human subjects, by electron paramagnetic resonance. *Adv Exp Med Biol* 361: 119–128, 1994.
32. Swartz HM, Boyer S, Brown D, Chang K, Gast P, Glockner JF, Hu H, Liu KJ, Moussavi M, Nilges M, and et al. The use of EPR for the measurement of the concentration of oxygen *in vivo* in tissues under physiologically pertinent conditions and concentrations. *Adv Exp Med Biol* 317: 221–228, 1992.
33. Swartz HM and Dunn JF. Measurements of oxygen in tissues: overview and perspectives on methods. *Adv Exp Med Biol* 530: 1–12, 2003.
34. Trochu JN, Bouhour JB, Kaley G, and Hintze TH. Role of endothelium-derived nitric oxide in the regulation of cardiac oxygen metabolism: implications in health and disease. *Circ Res* 87: 1108–1117, 2000.
35. Vinogradov AD and Grivennikova VG. Generation of superoxide-radical by the NADH:ubiquinone oxidoreductase of heart mitochondria. *Biochemistry (Mosc)* 70: 120–127, 2005.
36. Wang P and Zweier JL. Measurement of nitric oxide and peroxynitrite generation in the postischemic heart. Evidence for peroxynitrite-mediated reperfusion injury. *J Biol Chem* 271: 29223–29230, 1996.
37. Wolin MS, Xie YW, and Hintze TH. Nitric oxide as a regulator of tissue oxygen consumption. *Curr Opin Nephrol Hypertens* 8: 97–103, 1999.
38. Xie YW and Wolin MS. Role of nitric oxide and its interaction with superoxide in the suppression of cardiac muscle mitochondrial respiration. Involvement in response to hypoxia/reoxygenation. *Circulation* 94: 2580–2586, 1996.
39. Zhao H, Kalivendi S, Zhang H, Joseph J, Nithipatikom K, Vasquez–Vivar J, and Kalyanaraman B. Superoxide reacts with hydroethidine but forms a fluorescent product that is distinctly different from ethidium: potential implications in intracellular fluorescence detection of superoxide. *Free Radic Biol Med* 34: 1359–1368, 2003.
40. Zhao X, He G, Chen YR, Pandian RP, Kuppusamy P, and Zweier JL. Endothelium-derived nitric oxide regulates postischemic myocardial oxygenation and oxygen consumption by modulation of mitochondrial electron transport. *Circulation* 111: 2966–2972, 2005.
41. Zuo L, Christofi FL, Wright VP, Liu CY, Merola AJ, Berliner LJ, and Clanton TL. Intra- and extracellular measurement of reactive oxygen species produced during heat stress in diaphragm muscle. *Am J Physiol Cell Physiol* 279: C1058–1066, 2000.
42. Zuo L and Clanton TL. Detection of reactive oxygen and nitrogen species in tissues using redox-sensitive fluorescent probes. *Methods Enzymol* 352: 307–325, 2002.
43. Zuo L and Clanton TL. Reactive oxygen species formation in the transition to hypoxia in skeletal muscle. *Am J Physiol Cell Physiol* 289: C207–216, 2005.
44. Zweier JL and Kuppusamy P. Electron paramagnetic resonance measurements of free radicals in the intact beating heart: a technique for detection and characterization of free radicals in whole biological tissues. *Proc Natl Acad Sci USA* 85: 5703–5707, 1988.
45. Zweier JL and Kuppusamy P. *In vivo* EPR spectroscopy of free radicals in the heart. *Environ Health Perspect* 102 Suppl 10: 45–51, 1994.
46. Zweier JL, Kuppusamy P, and Lutty GA. Measurement of endothelial cell free radical generation: evidence for a central mechanism of free radical injury in postischemic tissues. *Proc Natl Acad Sci USA* 85: 4046–4050, 1988.
47. Zweier JL, Kuppusamy P, Thompson–Gorman S, Klunk D, and Lutty GA. Measurement and characterization of free radical generation in reoxygenated human endothelial cells. *Am J Physiol* 266: C700–708, 1994.

Address reprint requests to:
Guanglong He, Ph.D.
420 West 12th Avenue, 124A
Columbus, OH 43210

E-mail: Guanglong.He@osumc.edu

Date of first submission to ARS Central, July 17, 2006; date of final revised submission, November 13, 2006; date of acceptance, November 14, 2006.

This article has been cited by:

1. Denis A. Komarov, Ilirian Dhimitruka, Igor A. Kirilyuk, Dmitrii G. Trofimiov, Igor A. Grigor'ev, Jay L. Zweier, Valery V. Khramtsov. 2012. Electron paramagnetic resonance monitoring of ischemia-induced myocardial oxygen depletion and acidosis in isolated rat hearts using soluble paramagnetic probes. *Magnetic Resonance in Medicine* **68**:2, 649-655. [CrossRef]
2. Ricardo Quarrie, Daniel S. Lee, Gregory Steinbaugh, Brandon Cramer, Warren Erdahl, Douglas R. Pfeiffer, Jay L. Zweier, Juan A. Crestanello. 2012. Ischemic preconditioning preserves mitochondrial membrane potential and limits reactive oxygen species production. *Journal of Surgical Research* . [CrossRef]
3. M.G. Handley, R.A. Medina, E. Nagel, P.J. Blower, R. Southworth. 2011. PET imaging of cardiac hypoxia: Opportunities and challenges. *Journal of Molecular and Cellular Cardiology* . [CrossRef]
4. Kiyokazu Koga , Agnes Kenessey , Saul R. Powell , Cristina P. Sison , Edmund J. Miller , Kaie Ojamaa . 2011. Macrophage Migration Inhibitory Factor Provides Cardioprotection During Ischemia/Reperfusion by Reducing Oxidative Stress. *Antioxidants & Redox Signaling* **14**:7, 1191-1202. [Abstract] [Full Text HTML] [Full Text PDF] [Full Text PDF with Links]
5. Raffaella Rastaldo , Sandra Cappello , Anna Folino , Gianni Losano . 2011. Effect of Apelin-Apelin Receptor System in Postischaemic Myocardial Protection: A Pharmacological Postconditioning Tool?. *Antioxidants & Redox Signaling* **14**:5, 909-922. [Abstract] [Full Text HTML] [Full Text PDF] [Full Text PDF with Links]
6. Yuanjing Li, Ming Cai, Yi Xu, Harold M. Swartz, Guanglong He. 2011. Late phase ischemic preconditioning preserves mitochondrial oxygen metabolism and attenuates post-ischemic myocardial tissue hyperoxygenation. *Life Sciences* **88**:1-2, 57-64. [CrossRef]
7. Ricardo Quarrie, Brandon M. Cramer, Daniel S. Lee, Gregory E. Steinbaugh, Warren Erdahl, Douglas R. Pfeiffer, Jay L. Zweier, Juan A. Crestanello. 2011. Ischemic Preconditioning Decreases Mitochondrial Proton Leak and Reactive Oxygen Species Production in the Postischemic Heart1. *Journal of Surgical Research* **165**:1, 5-14. [CrossRef]
8. Tiewei Lu , Sampath Parthasarathy , Hong Hao , Min Luo , Shabnam Ahmed , Jing Zhu , Suxin Luo , Periannan Kuppusamy , Chandan K. Sen , Catherine M. Verfaillie , Jie Tian , Zhenguo Liu . 2010. Reactive Oxygen Species Mediate Oxidized Low-Density Lipoprotein-Induced Inhibition of Oct-4 Expression and Endothelial Differentiation of Bone Marrow Stem Cells. *Antioxidants & Redox Signaling* **13**:12, 1845-1856. [Abstract] [Full Text HTML] [Full Text PDF] [Full Text PDF with Links]
9. Zequan Yang, Victor E. Laubach, Brent A. French, Irving L. Kron. 2009. Acute hyperglycemia enhances oxidative stress and exacerbates myocardial infarction by activating nicotinamide adenine dinucleotide phosphate oxidase during reperfusion. *The Journal of Thoracic and Cardiovascular Surgery* **137**:3, 723-729. [CrossRef]
10. Hu Chen, Honglian Shi. 2008. A reducing environment stabilizes HIF-2# in SH-SY5Y cells under hypoxic conditions. *FEBS Letters* **582**:28, 3899-3902. [CrossRef]
11. Zita Hertelendi , Attila Tóth , Attila Borbély , Zoltán Galajda , Jolanda van der Velden , Ger J.M. Stienen , István Édes , Zoltán Papp . 2008. Oxidation of Myofilament Protein Sulfhydryl Groups Reduces the Contractile Force and Its Ca2+ Sensitivity in Human Cardiomyocytes. *Antioxidants & Redox Signaling* **10**:7, 1175-1184. [Abstract] [Full Text PDF] [Full Text PDF with Links]
12. Samarjit Das, Nadeem Khan, Subhendu Mukherjee, Debasis Bagchi, Narasimman Gurusamy, Harold Swartz, Dipak K. Das. 2008. Redox regulation of resveratrol-mediated switching of death signal into survival signal. *Free Radical Biology and Medicine* **44**:1, 82-90. [CrossRef]
13. Masaichi-Chang-il LEE. 2008. Biomedical Application of Electron Spin Resonance (ESR) Spectroscopy —Assessment of Antioxidant Property for Development of Drugs—. *YAKUGAKU ZASSHI* **128**:5, 753-763. [CrossRef]